

FLUID-SOLID COUPLED ANALYSIS BASED ON ALE GSMAC-FEM

G. Hashimoto* and T. Tanahashi†

*Keio University, Faculty of Science and Technology,
Hiyoshi 3-14-1, Kohoku-ku, Yokohama, Japan
e-mail: gakuhashimoto@2001.jukuin.keio.ac.jp

†Keio University, Faculty of Science and Technology,
Hiyoshi 3-14-1, Kohoku-ku, Yokohama, Japan
e-mail: takahiko@1964.jukuin.keio.ac.jp

Key words: Fluid-Solid Interaction, GSMAC-FEM, Hookean Elastic Material, Incompressible Hyperelastic Material, Vortex-induced Vibration

Abstract. *In the present study, the explicit computational method for fluid-solid coupled system is proposed based on ALE (Arbitrary Lagrangian-Eulerian) GSMAC(Generalized-Simplified Marker and Cell)-FEM suitable for low capacity and high speed computation in order to analyze the interaction of fluid and flexible rubber-like solid. The stability of time-marching is improved by satisfying the fluid-solid strongly coupled equation at next time using the explicit iterative calculation. Only the Poisson equation for the pressure correction is computed implicitly in this coupling method. In order to verify the effectiveness for the problem that the fluid-solid interaction is large, two-dimensional vortex-induced vibration problem is analyzed about the interaction of vortices and elastic plate attached to rigid prism.*

1 INTRODUCTION

In recent years, much attention has been paid to a fluid-solid coupled analysis. The deformation of solid wall which is caused by flow is one of important mechanical problems. The phenomenon becomes very complex, because solid wall influences the flow field. In the coupling phenomena of fluid and flexible rubber-like solid whose Young's modulus is small, the solid wall is deformed largely by flow force and the vibration with small frequency is caused.

It is necessary to evaluate the discretized equations of fluid and solid systems at next time in order to improve the stability of calculation for the case in which fluid and solid interact largely. The implicit method is often utilized for the time integration^{1,2}. However, the computer load is big for the matrix calculation in this method. It is possible to use explicit method for the time integration in order to reduce the computer load. Though

the explicit method is effective in flexible rubber-like solid analysis, the constraint of time step width becomes severe in the vibration with large frequency.

In the present study, the explicit computational method for fluid-solid coupled system is proposed using ALE (Arbitrary Lagrangian-Eulerian) GSMAC (Generalized-Simplified Marker and Cell)-FEM³ suitable for low capacity and high speed computation in order to analyze the interaction of fluid and flexible rubber-like solid. The stability of time-marching is improved by satisfying the fluid-solid strongly coupled equation at next time using the explicit iterative calculation. Only the Poisson equation is computed implicitly in this fluid-solid coupled method as well as the coupling method proposed by Ishihara and Yoshimura⁴. The velocity-pressure simultaneous relaxation method is used in GSMAC-FEM in order to leave out the process of making the non-diagonal component of the total coefficient matrix when the discretized Poisson equation is computed.

2 GOVERNING EQUATIONS

Figure 2 shows the fluid domain Ω_F , the solid domain Ω_S , and the interface Γ_I . The fluid is assumed to be incompressible Newtonian fluid, and the solid to be Hookean elastic material or incompressible hyperelastic material. ALE (Arbitrary Lagrangian-Eulerian) method for the fluid and Lagrangian method for the solid are made use of respectively.

The governing equations for incompressible Newtonian fluid in Ω_F are expressed as follows.

(Continuity Equation)

$$\nabla \cdot \mathbf{v} = 0 \quad (1a)$$

(Equations of Motion)

$$\rho \frac{\delta \mathbf{v}}{\delta t} + \rho(\mathbf{v} - \mathbf{w}) \cdot \nabla \mathbf{v} = -\nabla p + \nabla \cdot \boldsymbol{\tau} + \rho \mathbf{b} \quad (1b)$$

(The Relations between Viscous Stress and Velocity Gradient)

$$\boldsymbol{\tau} = \mu(\nabla \mathbf{v} + \mathbf{v} \overleftarrow{\nabla}) \quad (1c)$$

where ∇ is the nabla of spatial coordinates, \mathbf{v} is the velocity, ρ is the density, $\delta/\delta t = (\partial/\partial t)|_{\boldsymbol{\chi}}$ is the arbitrary time-derivative, \mathbf{w} is the arbitrary velocity, p is the pressure, $\boldsymbol{\tau}$ is the viscous stress tensor, \mathbf{b} is the volume force per unit mass, μ is the viscosity.

The governing equations for Hookean elastic material in Ω_S^0 are expressed as follows.
(Equations of Motion)

$$\rho^0 \frac{d^2 \mathbf{u}}{dt^2} = \nabla_X \cdot (\mathbf{S} \cdot \mathbf{F}^T) + \rho^0 \mathbf{b} \quad (2a)$$

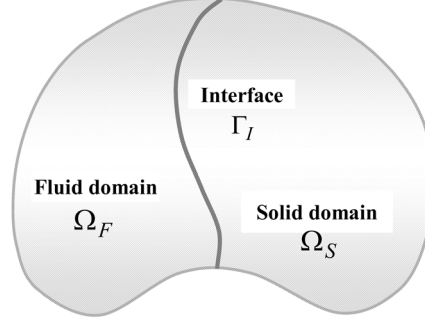


Figure 1: Fluid domain, solid domain, and the interface

(Constitutive Equations)

$$\mathbf{S} = \lambda_S (\text{tr} \mathbf{E}) \mathbf{I} + 2\mu_S \mathbf{E} \quad (2b)$$

(The Relations between Strain and Displacement Gradient)

$$\mathbf{E} = \frac{1}{2} (\nabla_X \mathbf{u} + \mathbf{u} \overleftarrow{\nabla}_X + \nabla_X \mathbf{u} \cdot \mathbf{u} \overleftarrow{\nabla}_X) \quad (2c)$$

where ρ^0 is the initial density, $d/dt = (\partial/\partial t)|_{\mathbf{X}}$ is the material time-derivative, \mathbf{u} is the displacement, ∇_X is the nable of material coordinates, \mathbf{S} is the 2nd Piola-Kirchhoff stress tensor, $\mathbf{F} = \mathbf{I} + \mathbf{u} \overleftarrow{\nabla}_X$ is the deformation gradient tensor, \mathbf{E} is the Green-Lagrange strain tensor, λ_S and μ_S are the Lamé constants, and \mathbf{I} is the identity tensor. Lamé constants are expressed as follows.

$$\lambda_S = \frac{E_S \nu_S}{(1 + \nu_S)(1 - 2\nu_S)} \quad (3a)$$

$$\mu_S = \frac{E_S}{2(1 + \nu_S)} \quad (3b)$$

where E_S is Young's modulus and ν_S is Poisson's ratio.

The governing equations for incompressible hyperelastic material in Ω_S are expressed as follows.

(Continuity Equation)

$$\nabla \cdot \mathbf{v} = 0 \quad (4a)$$

(Equations of Motion)

$$\rho \frac{d\mathbf{v}}{dt} = -\nabla p_r + \nabla \cdot \boldsymbol{\tau} + \rho \mathbf{b} \quad (4b)$$

(The Relations between Displacement and Velocity)

$$\frac{d\mathbf{u}}{dt} = \mathbf{v} \quad (4c)$$

(Transformation Equation of Pressure)

$$p_r = p + \frac{2}{3} \left[\frac{\partial W}{\partial \tilde{I}_B} (\text{tr} \mathbf{B}) + \frac{\partial W}{\partial \tilde{II}_B} \{ (\text{tr} \mathbf{B})^2 - \text{tr}(\mathbf{B} \cdot \mathbf{B}) \} \right] \quad (4d)$$

(The Relations between Extra Stress and Deformation)

$$\boldsymbol{\tau} = 2 \left\{ \frac{\partial W}{\partial \tilde{I}_B} + \frac{\partial W}{\partial \tilde{II}_B} (\text{tr} \mathbf{B}) \right\} \mathbf{B} - 2 \frac{\partial W}{\partial \tilde{II}_B} \mathbf{B} \cdot \mathbf{B} \quad (4e)$$

where p_r is the transformed pressure, $\boldsymbol{\tau}$ is the extra stress, $\mathbf{B} = \mathbf{F} \cdot \mathbf{F}^T$ is the left Cauchy-Green deformation tensor, W is the strain energy density per unit original volume, $\tilde{I}_B = I_B/III_B^{1/3}$ and $\tilde{II}_B = II_B/III_B^{2/3}$ are the reduced invariants of \mathbf{B} , I_B , II_B , and III_B are invariants of \mathbf{B} . Although $\det \mathbf{F} = 1$ or $III_B = 1$ is usually used as the incompressibility constraint condition in mixed FEM analysis of incompressible hyperelastic material, the continuity equation (4a) is used to obtain velocity-pressure decoupled FEM formulations^{5,6}. W is approximated as polynomial.

$$\begin{aligned} W = & c_{10}(\tilde{I}_B - 3) + c_{01}(\tilde{II}_B - 3) + c_{11}(\tilde{I}_B - 3)(\tilde{II}_B - 3) \\ & + c_{20}(\tilde{I}_B - 3)^2 + c_{02}(\tilde{II}_B - 3)^2 \\ & + c_{21}(\tilde{I}_B - 3)^2(\tilde{II}_B - 3) + c_{12}(\tilde{I}_B - 3)(\tilde{II}_B - 3)^2 \\ & + c_{30}(\tilde{I}_B - 3)^3 + c_{03}(\tilde{II}_B - 3)^3 \end{aligned} \quad (5)$$

where c_{mn} ($m, n = 0, 1, 2, 3$) is the material constants of Mooney-Rivlin model.

The boundary condition on Γ_I is expressed as follows.

(Compatibility)

$$\mathbf{v}|_{\text{Fluid}} = \frac{d\mathbf{u}}{dt}|_{\text{Solid}} \quad (6a)$$

(Equilibrium)

$$(\mathbf{n} \cdot \mathbf{T})|_{\text{Fluid}} + (\mathbf{n} \cdot \mathbf{T})|_{\text{Solid}} = \mathbf{0} \quad (6b)$$

where \mathbf{n} is the outward normal vector and \mathbf{T} is the Cauchy stress tensor.

3 COMPUTATIONAL METHOD

3.1 Derivation of fluid-solid coupled equations

The fluid-solid strongly coupled equations are derived according to the following procedure.

- (1) The explicit iterative calculation is applied to the time discretization of the fluid and the solid from the idea of Newmark- β method in order to solve oscillation problems accurately.
- (2) For the fluid, the decoupled equations consisting of the predictor step equations, the Poisson equation, and the corrector step equations are derived so as to satisfy the continuity equation at the next time. For the incompressible hyperelastic material, the decoupled equations are similarly derived.
- (3) The temporal discretized equations of the fluid and the solid are discretized spatially using Galerkin FEM respectively. Then the velocity-pressure simultaneous relaxation iteration is introduced for the fluid and it is similarly introduced for the incompressible hyperelastic material using GSMAC-FEM.
- (4) The predictor step equations for the fluid and the equations of motion for Hookean elastic material, or the predictor step equations for the fluid and incompressible hyperelastic material are combined into the fluid-solid strongly coupled equations using the compatibility and equilibrium conditions given on Γ_I .

3.2 Algorithm of the fluid-solid coupled analysis

Figure 2 shows the flowchart of the ALE GSMAC-FEM including the above computational method. The algorithm is the double iterative calculation consisting of the explicit iteration located outside and the velocity-pressure simultaneous relaxation iteration located inside. i is the velocity or displacement node and l is the pressure node in this figure. \tilde{D}_l is the node average of $\nabla \cdot \mathbf{v}$, and ϵ_1 is the convergence criterion of simultaneous relaxation iteration in Figure 2 (b).

The coupled analysis of incompressible Newtonian fluid and Hookean elastic material is implemented according to the following procedure. The representative variable of the fluid is $\{\mathbf{v}, p, \mathbf{w}\}$ and that of Hookean elastic material is $\{\mathbf{u}\}$. The fluid variable is $\{\mathbf{v}\}$ and the solid variable is $\{\mathbf{u}\}$ on Γ_I .

- (1) $\{\mathbf{u}^n\}$ in Ω_S^0 , $\{\mathbf{v}^n, p^n, \mathbf{w}^n\}$ in Ω_F^n , and $\{\mathbf{u}^n, \mathbf{v}^n\}$ on Γ_I^n are known at time $t = t^n$.
- (2) The explicit iteration is set at $m = 0$. Then $\{\mathbf{u}^{(0)}\} = \{\mathbf{u}^n\}$ in Ω_S^0 , $\{\mathbf{v}^{(0)}, p^{(0)}, \mathbf{w}^{(0)}\} = \{\mathbf{v}^n, p^n, \mathbf{w}^n\}$ in $\Omega_F^{(0)}$, and $\{\mathbf{u}^{(0)}, \mathbf{v}^{(0)}\} = \{\mathbf{u}^n, \mathbf{v}^n\}$ on $\Gamma_I^{(0)}$.
- (3) After calculating of the fluid-solid coupled equations, $\{\mathbf{u}^{(m+1)}\}$ in Ω_S^0 , $\{\tilde{\mathbf{v}}, p^{(m)}, \mathbf{w}^{(m)}\}$ in $\Omega_F^{(m)}$, and $\{\mathbf{u}^{(m+1)}, \mathbf{v}^{(m+1)}\}$ on $\Gamma_I^{(m)}$ are obtained.

- (4) The velocity-pressure simultaneous relaxation iteration is calculated in $\Omega_F^{(m)}$. The fluid velocity $\tilde{\mathbf{v}}$ and the fluid pressure $p^{(m)}$ are corrected, and then $\{\mathbf{v}^{(m+1)}, p^{(m+1)}, \mathbf{w}^{(m)}\}$ in $\Omega_F^{(m)}$ is obtained.
- (5) Because the fluid mesh velocity $\mathbf{w}^{(m+1)}$ is decided from the interface velocity $\mathbf{v}^{(m+1)}$, $\{\mathbf{v}^{(m+1)}, p^{(m+1)}, \mathbf{w}^{(m+1)}\}$ in $\Omega_F^{(m)}$ is obtained.
- (6) If $|\mathbf{v}^{(m+1)} - \mathbf{v}^{(m)}| \leq \epsilon_2$, then $\{\mathbf{u}^{n+1}\} = \{\mathbf{u}^{(m+1)}\}$ in Ω_S^0 , $\{\mathbf{v}^{n+1}, p^{n+1}, \mathbf{w}^{n+1}\} = \{\mathbf{v}^{(m+1)}, p^{(m+1)}, \mathbf{w}^{(m+1)}\}$ in $\Omega_F^{(m)}$, and $\{\mathbf{u}^{n+1}, \mathbf{v}^{n+1}\} = \{\mathbf{u}^{(m+1)}, \mathbf{v}^{(m+1)}\}$ on $\Gamma_I^{(m)}$. If $|\mathbf{v}^{(m+1)} - \mathbf{v}^{(m)}| > \epsilon_2$, then $(m+1) \rightarrow (m)$, and the procedure from (3) to (6) is iterated.

The coupled analysis of incompressible Newtonian fluid and hyperelastic material is implemented according to the following procedure. The representative variable of the fluid is $\{\mathbf{v}, p, \mathbf{w}\}$ and that of incompressible hyperelastic material is $\{\mathbf{u}, \mathbf{v}, p_r\}$. The fluid variable is $\{\mathbf{v}\}$ and the solid variable is $\{\mathbf{u}, \mathbf{v}\}$ on Γ_I .

- (1) $\{\mathbf{u}^n, \mathbf{v}^n, p_r^n\}$ in Ω_S^n , $\{\mathbf{v}^n, p^n, \mathbf{w}^n\}$ in Ω_F^n , and $\{\mathbf{u}^n, \mathbf{v}^n\}$ in Γ_I^n are known at time $t = t^n$.
- (2) The explicit iteration is set at $m = 0$. Then $\{\mathbf{u}^{(0)}, \mathbf{v}^{(0)}, p_r^{(0)}\} = \{\mathbf{u}^n, \mathbf{v}^n, p_r^n\}$ in $\Omega_S^{(m)}$, $\{\mathbf{v}^{(0)}, p^{(0)}, \mathbf{w}^{(0)}\} = \{\mathbf{v}^n, p^n, \mathbf{w}^n\}$ in $\Omega_F^{(m)}$, and $\{\mathbf{u}^{(0)}, \mathbf{v}^{(0)}\} = \{\mathbf{u}^n, \mathbf{v}^n\}$ on $\Gamma_I^{(m)}$.
- (3) After calculating of the fluid-solid coupled equations, $\{\mathbf{u}^{(m)}, \tilde{\mathbf{v}}, p_r^{(m)}\}$ in $\Omega_S^{(m)}$, $\{\tilde{\mathbf{v}}, p^{(m)}, \mathbf{w}^{(m)}\}$ in $\Omega_F^{(m)}$, and $\{\mathbf{u}^{(m)}, \tilde{\mathbf{v}}\}$ on $\Gamma_I^{(m)}$ are obtained.
- (4) The velocity-pressure simultaneous relaxation iteration is calculated in $\Omega_S^{(m)}$. The solid velocity $\tilde{\mathbf{v}}$ and the solid transformed pressure $p_r^{(m)}$ are corrected. Then $\{\mathbf{u}^{(m+1)}, \mathbf{v}^{(m+1)}, p_r^{(m+1)}\}$ in $\Omega_S^{(m)}$ and $\{\mathbf{u}^{(m+1)}, \mathbf{v}^{(m+1)}\}$ on $\Gamma_I^{(m)}$ are obtained.
- (5) The velocity-pressure simultaneous relaxation iteration is calculated in $\Omega_F^{(m)}$. The fluid velocity $\tilde{\mathbf{v}}$ and the fluid pressure $p^{(m)}$ are corrected. Then $\{\mathbf{v}^{(m+1)}, p^{(m+1)}, \mathbf{w}^{(m)}\}$ in $\Omega_F^{(m)}$ is also obtained.
- (6) Because the fluid mesh velocity $\mathbf{w}^{(m+1)}$ is decided from the interface velocity $\mathbf{v}^{(m+1)}$, $\{\mathbf{v}^{(m+1)}, p^{(m+1)}, \mathbf{w}^{(m+1)}\}$ in $\Omega_F^{(m)}$ is obtained.
- (7) If $|\mathbf{v}^{(m+1)} - \mathbf{v}^{(m)}| \leq \epsilon_2$, then $\{\mathbf{u}^{n+1}, \mathbf{v}^{n+1}, p_r^{n+1}\} = \{\mathbf{u}^{(m+1)}, \mathbf{v}^{(m+1)}, p_r^{(m+1)}\}$ in $\Omega_S^{(m)}$, $\{\mathbf{v}^{n+1}, p^{n+1}, \mathbf{w}^{n+1}\} = \{\mathbf{v}^{(m+1)}, p^{(m+1)}, \mathbf{w}^{(m+1)}\}$ in $\Omega_F^{(m)}$, and $\{\mathbf{u}^{n+1}, \mathbf{v}^{n+1}\} = \{\mathbf{u}^{(m+1)}, \mathbf{v}^{(m+1)}\}$ on $\Gamma_I^{(m)}$. If $|\mathbf{v}^{(m+1)} - \mathbf{v}^{(m)}| > \epsilon_2$, then $(m+1) \rightarrow (m)$, and the procedure from (3) to (7) is iterated.

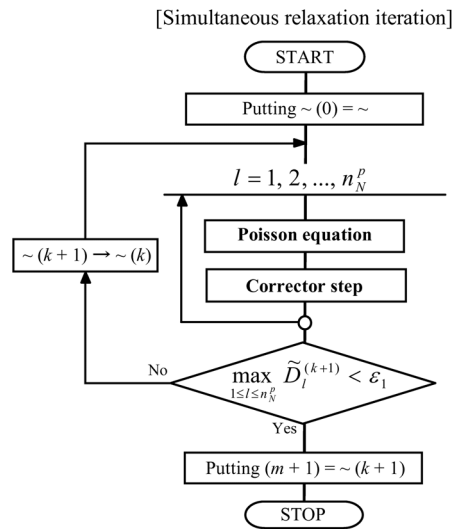
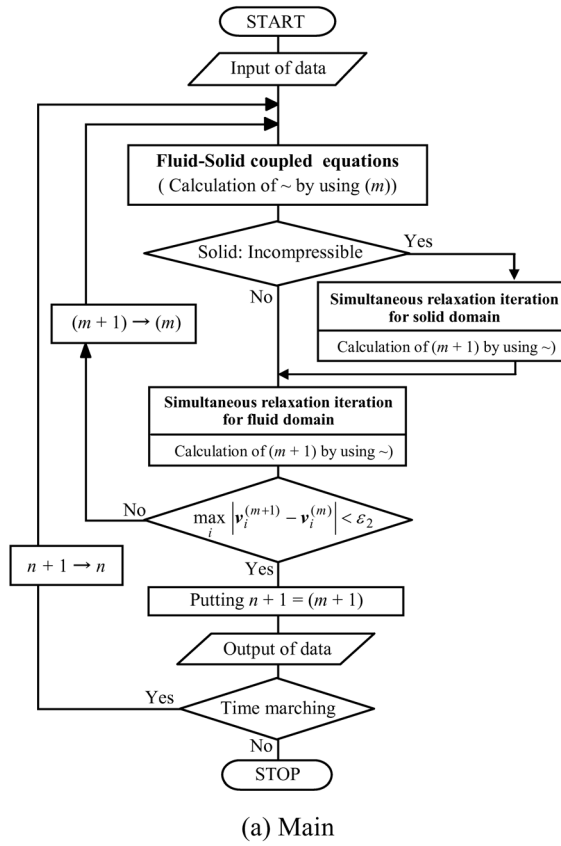


Figure 2: The flowchart of ALE GSMAC-FEM algorithm for analyzing fluid-solid coupled system

4 NUMERICAL EXAMPLES

Vortex-induced vibration is the forced oscillation caused by the unsteady hydrodynamic force of vortices shed from solid. In order to verify the effectiveness for the problem that the fluid-solid interaction is large, two-dimensional vortex-induced vibration problem is analyzed about the interaction of vortices and elastic plate attached to rigid prism.

Figure 3 shows the analysis model and the boundary conditions. Air flows impulsively at the inlet of the model as the initial condition. In this analysis, the elastic plate attached to the rigid prism is regarded as Hookean elastic material or incompressible hyperelastic material. Table 4 shows the physical properties of air, Hookean elastic material, incompressible hyperelastic material. Reynolds number $Re = L_r V_r / (\mu / \rho)$ is about 332 for the flow field. The first-order element and second-order element are used for the fluid velocity and the solid displacement so as to compare the results (see Figure 4). Figure 5 shows the analysis meshes. The total number of the degrees of freedom for the fluid velocity and the solid displacement in Mesh A is the same as Mesh B. In Mesh C, the elements of the elastic plate in Mesh B are divided into halves axially. The constraint of the solid time width becomes severer than that of the fluid time width. The time width in Mesh A and Mesh B is 1.0×10^{-5} s and that in Mesh C is 5.0×10^{-6} s to catch the wave propagated in solid elements sufficiently. The fluid mesh velocity is changed linearly from elastic plate surface to the outside boundary of the fluid domain. The convergence criterion of the simultaneous relaxation iteration is set at $\epsilon_1 = 1.0 \times 10^{-3} V_r / L_r$, and the convergence criterion of the explicit iteration at $\epsilon_2 = 1.0 \times 10^{-6} V_r$.

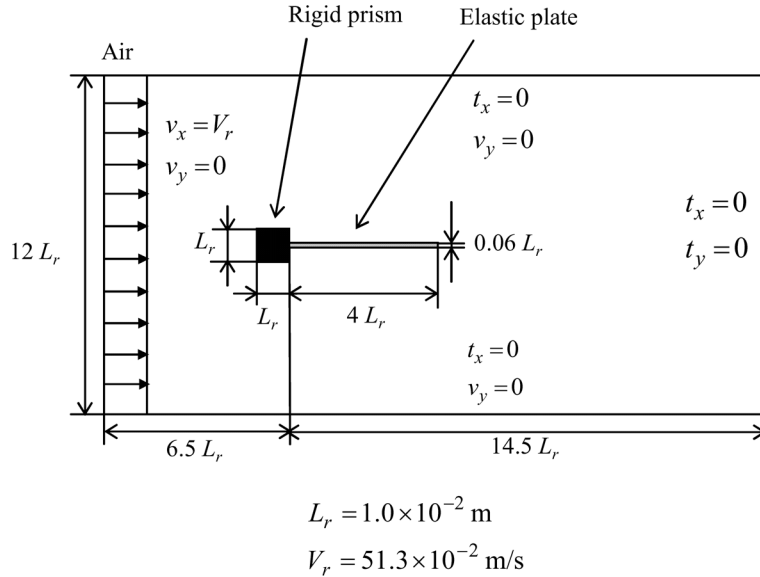


Figure 3: Analysis model and boundary conditions

(a) Incompressible Newtonian fluid (air)

ρ	1.18 kg/m^3
μ	$1.82 \times 10^{-5} \text{ Pa}$

(b) Hookean elastic material

ρ^0	$2.0 \times 10^3 \text{ kg/m}^3$
E_S	$2.0 \times 10^5 \text{ Pa}$
ν_S	0.35

(c) Incompressible hyperelastic material

ρ	$1.0 \times 10^3 \text{ kg/m}^3$
c_{10}	$1.81222092 \times 10^5 \text{ Pa}$
c_{01}	$9.95175450 \times 10^3 \text{ Pa}$
c_{11}	$-1.51094601 \times 10^2 \text{ Pa}$
c_{20}	$-2.11709610 \times 10^3 \text{ Pa}$
c_{02}	0.0
c_{21}	0.0
c_{12}	0.0
c_{30}	$5.00884866 \times 10^1 \text{ Pa}$
c_{03}	0.0

Table 1: Calculation data

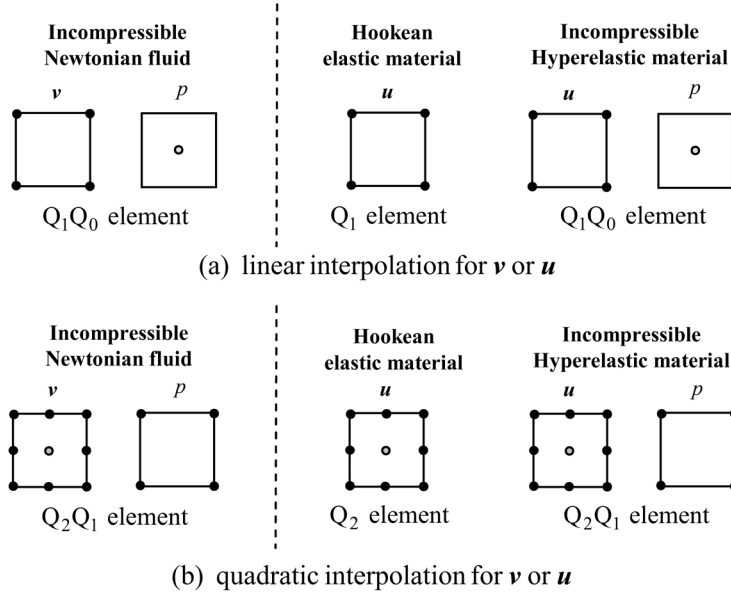
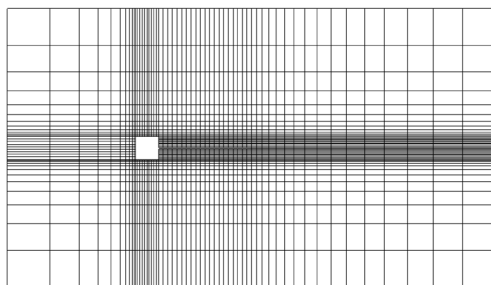
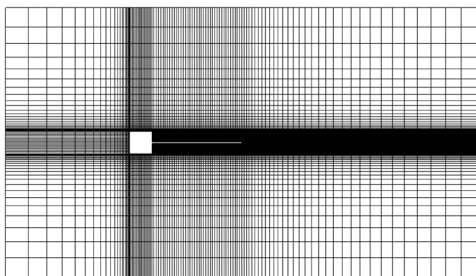


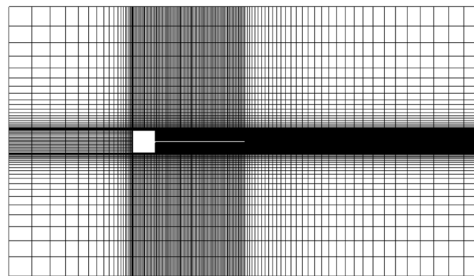
Figure 4: Quadrilateral elements for analyzing fluid-solid coupled system



(a) Mesh A (quadratic interpolation for \mathbf{v} or \mathbf{u} ;
fluid : 2170 elements, solid : 20 elements)



(b) Mesh B (linear interpolation for \mathbf{v} or \mathbf{u} ;
fluid : 8680 elements, solid : 40×2 elements)



(c) Mesh C (linear interpolation for \mathbf{v} or \mathbf{u} ;
fluid : 12200 elements, solid : 80×2 elements)

Figure 5: Analysis meshes

4.1 Hookean elastic material and air

The proposed computational method is evaluated from the coupled analysis results of Hookean elastic material and air. The obtained results are compared with the results using weakly coupling method which receives the data in the interface by Wall *et al.*⁷. The elements used by Wall *et al.* are Q_1Q_1 for fluid and Q_2 for solid. In Mesh A and Mesh B, the total number of the degrees of freedom for the displacement is the same as that by Wall *et al.* and the total number of the degrees of freedom for the fluid velocity is more than that by Wall *et al.*

Symmetric vortices arise from the rigid prism after the start of computation. After that, the flow field becomes asymmetric and vortices are shed one after another. The elastic plate begins to vibrate by the difference of hydrodynamic forces acting on the sides of it. Figure 6 and Figure 7 show the pressure contours in Mesh A and Mesh C respectively, and Figure 8 shows the time histories of the displacement at the elastic plate tip. Though the deformed shapes of the elastic plate are different, the obtained first-mode frequency is close to that by Wall *et al.* The influence of the second-mode frequency is

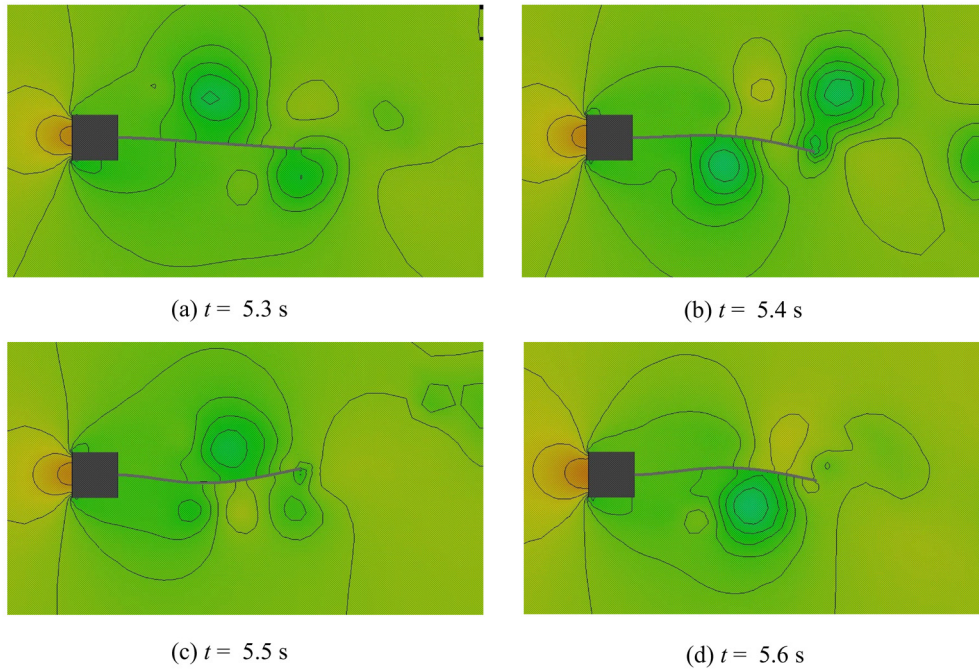


Figure 6: Pressure contours (Mesh A, fluid: Q_2Q_1 element, solid: Q_2 element)

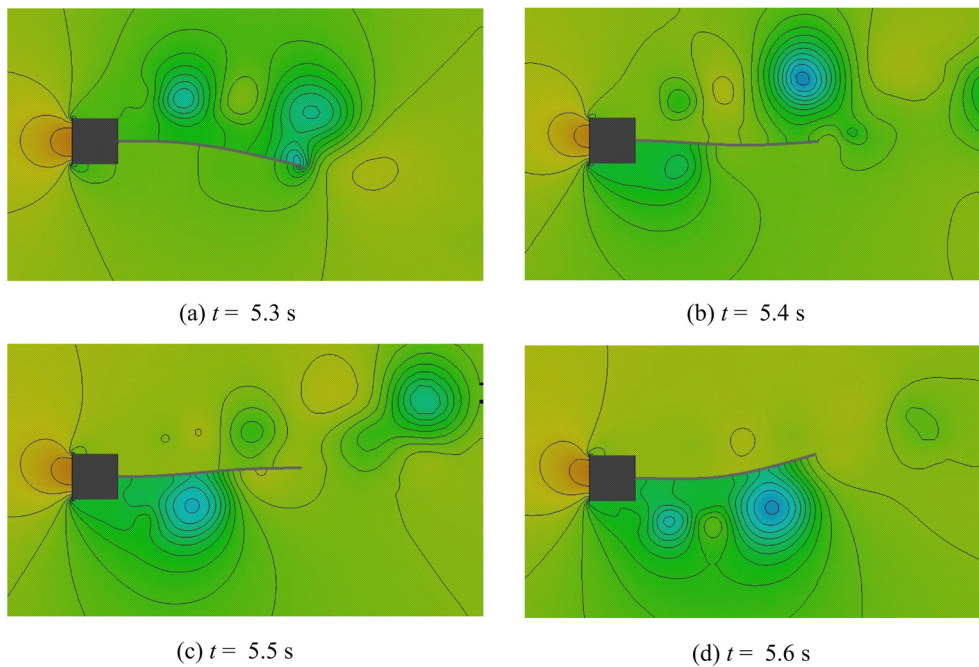


Figure 7: Pressure contours (Mesh C, fluid: Q_1Q_0 element, solid: Q_1 element)

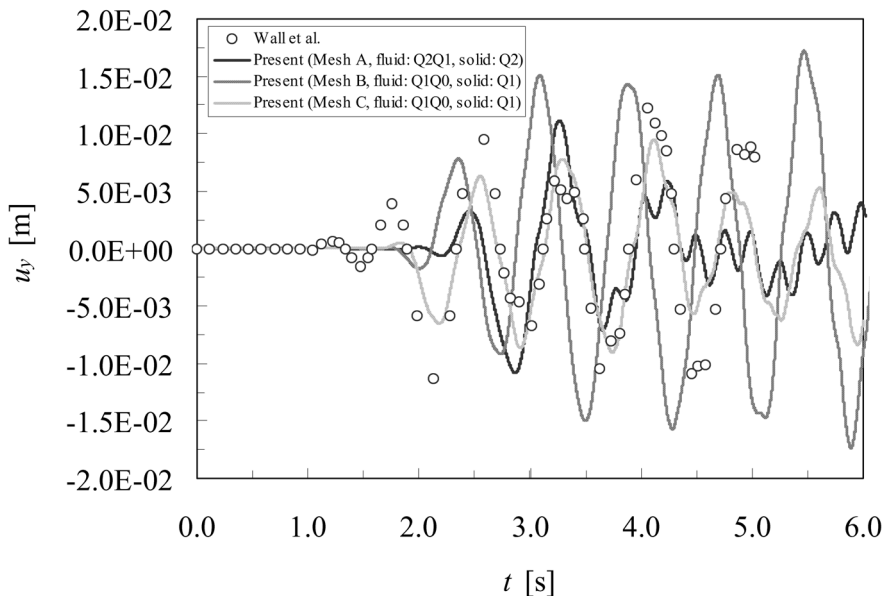


Figure 8: Time histories of displacement at the tip of elastic plate

small in Mesh B, while the influence of the second-mode frequency becomes larger and that of the first-mode frequency becomes smaller by increasing the total number of elements in Mesh C. The influence of second-mode frequency also increases by changing first-order elements to second-order in Mesh A. This is caused by shear locking of the obtained solutions by using linear elements.

4.2 Incompressible hyperelastic material and air

The computational method for the fluid and the solid which have incompressibility constraint conditions is evaluated from the coupled analysis of incompressible hyperelastic material and air. The elastic plate begins to vibrate by the difference of hydrodynamic forces as well as the plate made in Hookean elastic plate after the start of computation. Figure 9 and Figure 10 show the pressure contours in Mesh A and Mesh C respectively, and Figure 11 shows the time histories of the displacement at the elastic plate tip. The solutions become stiffing because of shear locking by using of linear elements for solid displacement in Mesh B. However it is possible to avoid locking by using of quadratic elements in Mesh A. By increasing the element number axially in Mesh C, the influence of shear locking is small, the results is close to the results in Mesh A. Figure 12 shows the time histories of the total area of solid domain. The variation of the total area is within $3.5 \times 10^{-5} \%$ and is very small because the incompressible constraint condition is fulfilled.

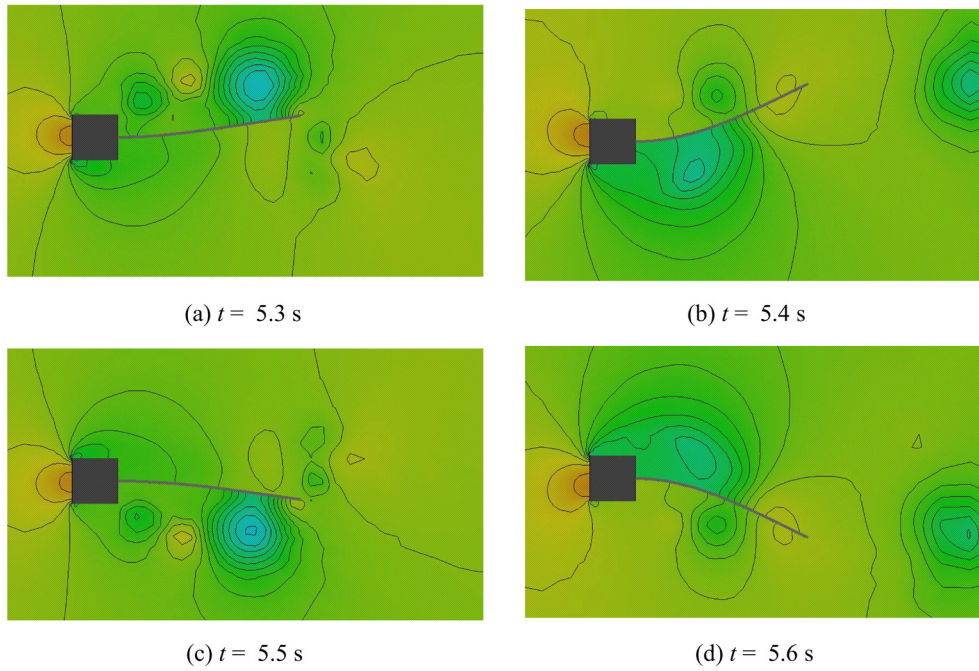


Figure 9: Pressure contours (Mesh A, fluid: Q_2Q_1 element, solid: Q_2Q_1 element)

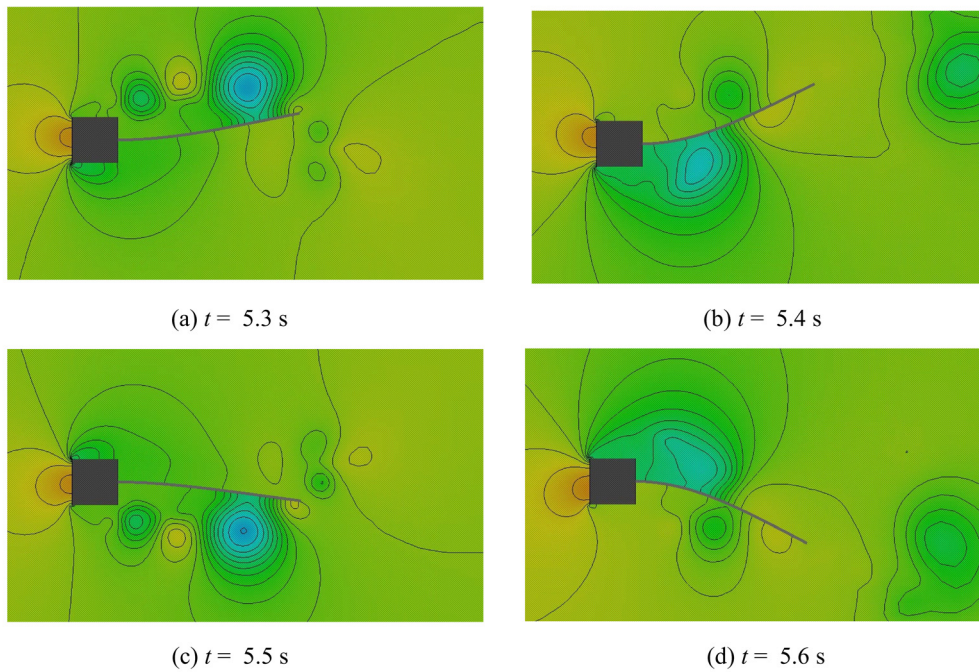


Figure 10: Pressure contours (Mesh C, fluid: Q_1Q_0 element, solid: Q_1Q_0 element)

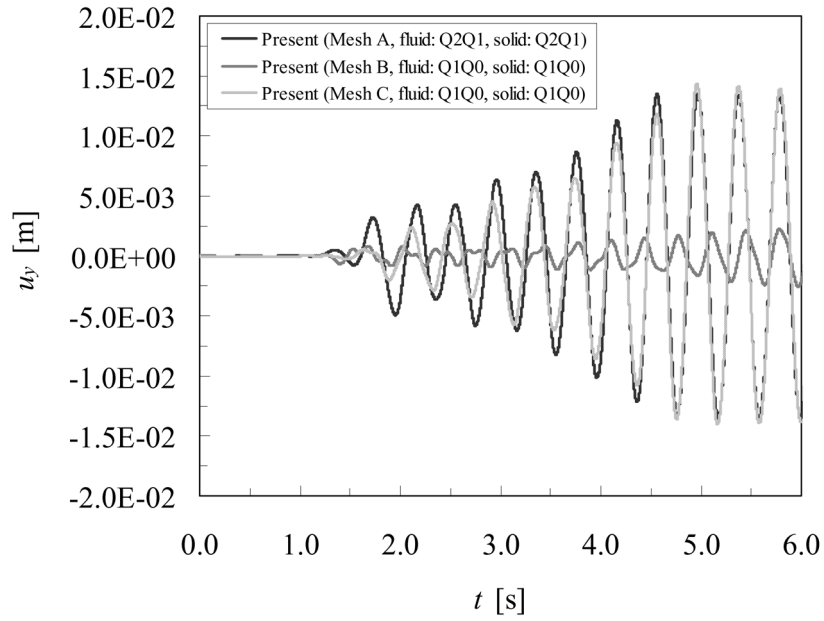


Figure 11: Time histories of displacement at the tip of elastic plate

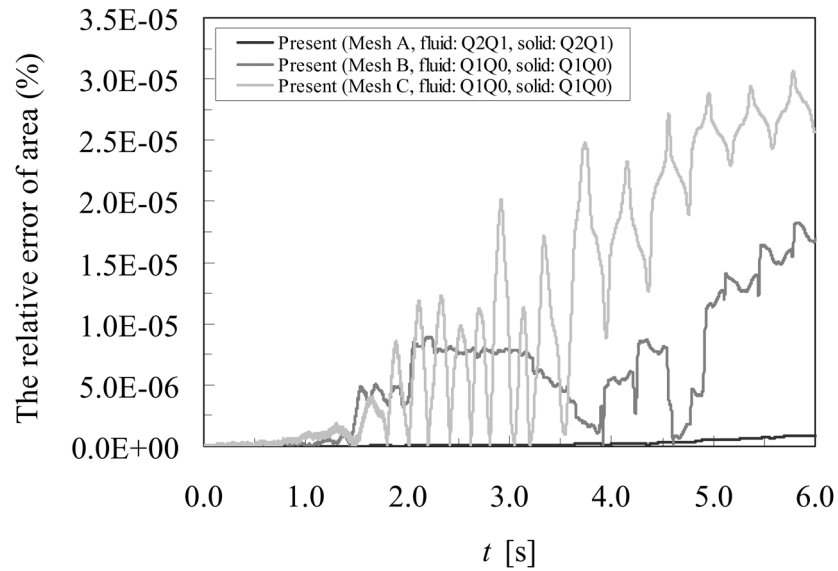


Figure 12: Time histories of the area of total solid domain

The comparisons with other strongly coupling methods are required for computation time and memory capacity in order to show the advantage of the present coupling method clearly.

5 CONCLUSIONS

In the present study, the computational method that is effective in the coupled analysis of fluid and flexible rubber-like solid was proposed based on ALE GSMAC-FEM suitable for high speed computation and low memory capacity. In order to verify the effectiveness for the problem that the fluid-solid interaction is large, two-dimensional vortex-induced vibration problem was analyzed about the interaction of vortices and elastic plate attached to rigid prism. When vortices were shed one after another from the prism, the plate began to vibrate by the difference of hydrodynamic forces acting on the sides of it. From the conservation of the total area of incompressible hyperelastic material, fluid-solid interaction imposed the incompressibility constraint condition was analyzed using GSMAC-FEM.

REFERENCES

- [1] S. Rugonyi and K.J. Bathe. On finite element analysis of fluid flows fully coupled with structural interactions. *CMES*, **2-2**, 195–212, (2001).
- [2] Q. Zhang and T. Hisada. Investigation of the coupling methods for FSI analysis by FEM. *Trans. Jpn. Soc. Mech. Eng.*, (in Japanese), **67-662**, 1555–1562, A (2001).
- [3] T. Tanahashi, H. Okanaga, and T. Saito. GSMAC finite element method for unsteady incompressible Navier-Stokes equations at high Reynolds numbers. *Int. J. Numer. Meths. Fluids*, **11**, 479–499, (1990).
- [4] D. Ishihara and S. Yoshimura. A monolithic approach for interaction of incompressible viscous fluid and elastic body based on fluid pressure Poisson equation. *Int. J. Num. Meths. Engng.*, **64**, 167–203, (2005).
- [5] G. Hashimoto and T. Tanahashi. A study of decoupled FEM for incompressible hyperelastic material (GSMAC-FEM analysis of Mooney-Rivlin material). *Trans. JSCEs*, (in Japanese), Paper No. 20040016, 1–8, (2004).
- [6] G. Hashimoto and T. Tanahashi. Investigation toward practical use into incompressible hyperelastic material analysis using GSMAC-FEM (application of higher-order elements and introduction of stiffening property). *Trans. JSCEs*, (in Japanese), Paper No. 20060001, 1–13, (2006).
- [7] W.A. Wall and E. Ramm. Fluid-structure interaction based upon a stabilized (ALE) finite element method. *Comput. Mech.*, (Proceedings of WCCM IV), 1–20, (1998).